07.2;07.3

Analysis of internal optical loss of 1.3 μm vertical-cavity surface-emitting laser based on n^{++}-InGaAs/p^{++}-InGaAs/p^{++}-InAlGaAs tunnel junction

© S.A. Blokhin[1], M.A. Bobrov[1], A.A. Blokhin[1], N.A. Maleev[1], A.G. Kuzmenkov[2], A.P. Vasyl'ev[2], S.S. Rochas[3], A.V. Babichev[3], I.I. Novikov[3], L.Ya. Karachinsky[3], A.G. Gladyshev[4], D.V. Denisov[5], K.O. Voropaev[6], A.Yu. Egorov[4], V.M. Ustinov[2]

[1] Ioffe Institute, St. Petersburg, Russia
[2] Submicron Heterostructures for Microelectronics, Research and Engineering Center, Russian Academy of Sciences, St. Petersburg, Russia
[3] ITMO University, St. Petersburg, Russia
[4] Connector Optics LLC, St. Petersburg, Russia
[5] St. Petersburg State Electrotechnical University „LETI", St. Petersburg, Russia
[6] OAO OKB-Planeta, Veliky Novgorod, Russia
E-mail: blokh@mail.ioffe.ru

Received June 25, 2021
Revised July 23, 2021
Accepted July 24, 2021

The analysis of internal optical loss and internal quantum efficiency in 1.3 μm-range InAlGaAsP/AlGaAs a composite n^+-InGaAs/p^+-InGaAs/p^+-InAlGaAs tunnel junction obtained in the frame of molecular-beam epitaxy and wafer fusion technology. The level of internal optical losses in the lasers under study was varied by depositing a dielectric layer on the surface of the output mirror. It is shown that it is possible in principle to achieve low internal optical loss of less than 0.08% and 0.14% per one pass (round-trip) at temperatures of 20°C and 90°C, respectively.

Keywords: vertical-cavity surface-emitting laser, wafer fusion, tunnel junction, superlattice, internal optical loss.

DOI: 10.21883/TPL.2022.15.53808.18938

In recent years, long-wavelength Vertical Cavity Surface-Emitting Lasers (VCSELs) have been considered as promising sources of optical radiation not only for information & telecommunication communication systems, but also for various types of sensors and microwave photonics devices, but also for sensors of various types and devices of microwave photonics, as well as hybrid integration with photonic integrated circuits [1]. The geometry of a VCSEL microcavity with carrier injection through intracavity contact (IC) layers and a tunnel junction (TJ) makes it possible to solve a number of fundamental problems inherent in long-wavelength VCSELs [2]. However, a significant achievement has become possible only for hybrid designs of VCSELs with distributed Bragg reflectors (DBR), which have high thermal conductivity and high reflectivity, in combination with the concept of the burried tunnel junction (BTJ). The most promising approaches include the hybrid integration of the short InGaAlAsP/InP optical cavity with high-contrast dielectric DBRs [3] and the fusion technology of the InGaAlAsP/InP optical cavity wafer with two AlGaAs/GaAs DBR wafers (hereinafter WF-VCSEL) [4], combining the advantages of the InGaAlAsP/InP and AlGaAs/GaAs material systems. In the design of such VCSELs, the n^+/p^+-InAlGaAs TJ is widely used to reduce the level of optical losses, which makes it impossible to heal the surface relief formed in the TJ layers within the framework of the molecular-beam epitaxy technology. Relatively recently, we have shown the possibility in principle for effective application of the molecular beam epitaxy method at all stages of the epitaxial growth of long-wavelength VCSEL heterostructures [5]. In addition, effective WF-VCSELs in the 1.3 μm spectral range based on short-period superlattice of InGaAs/InGaAlAs were presented [6].

This work presents the analysis results for the level of internal optical losses and the efficiency of current injection in a WF-VCSEL of the spectral range 1.3 μm with composite TJ n^+-InGaAs/p^+- InGaAs/p^+-InAlGaAs.

The heterostructure of the WF-VCSELs under study in the spectral range 1.3 μm consists of the lower DBR based on 35.5 pairs of $Al_{0.91}Ga_{0.09}As$/GaAs, the lower IC-layer *n*-InP with *n*-InGaAs contact layer, optical cavity containing the superlattice of $In_{0.6}Ga_{0.4}As/In_{0.53}Ga_{0.27}Al_{0.2}As$ (24 pairs, thicknesses 0.6 and 2.1 nm, respectively), *p*-InAlAs emitter and BTJ of n^+-InGaAs/p^+-InGaAs/p^+-InAlGaAs, upper IC-layer *n*-InP, and upper DBR based on 21.5 pairs of $Al_{0.91}Ga_{0.09}As$/GaAs. Figure 1 shows the intensity distribution of the electromagnetic field of the fundamental mode, the profiles of the refraction index and the doping level in the longitudinal direction. To minimize optical losses caused by absorption on free carriers, interband absorption, and scattering of light at sintered interfaces, IC-layers have the modulated doping profile, with high doping regions, the contact layer, TJ layers, and sintering boundaries located in the minima of the electromagnetic field. GaAs quarter-wave layers adjacent to the optical cavity lead to the increase in the total thickness of the optical cavity to 3λ, which,

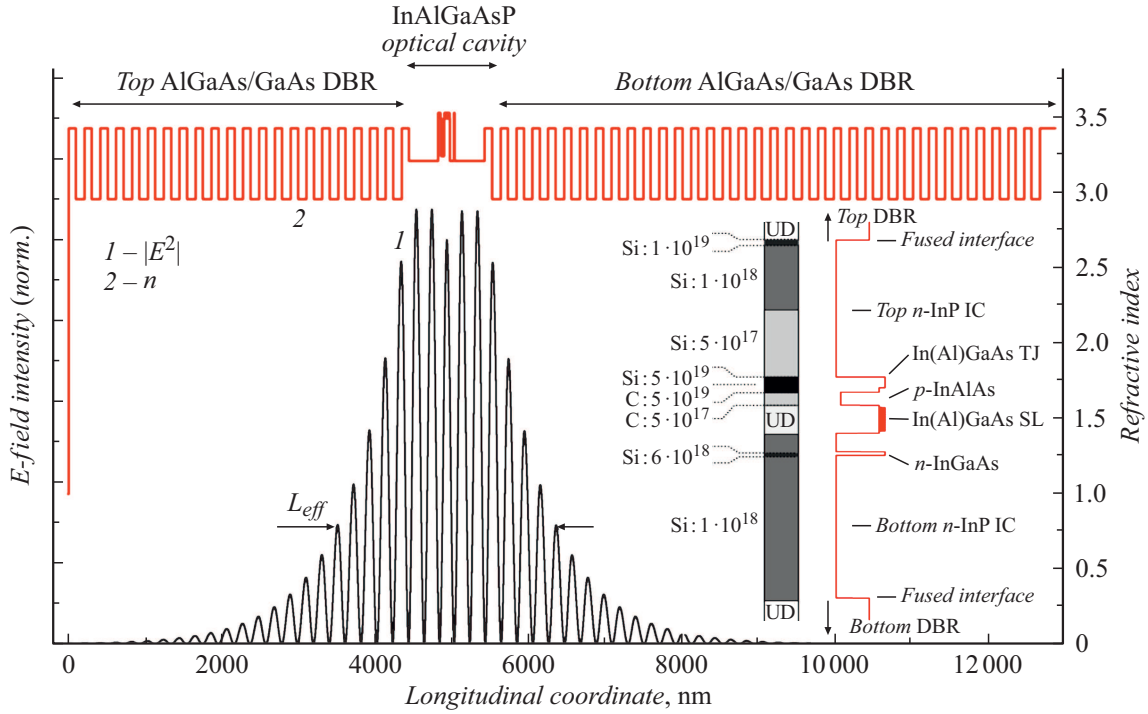

Figure 1. Intensity distribution of the electromagnetic field of the fundamental mode $|E^2|$ and the doping level (in cm^{-3}) of the structure along the profile of the refraction index n of the investigated VCSEL. The inset shows the higher magnification in the microcavity region. DBR — distributed Bragg reflector, IC — intracavity contact, TJ — tunnel junction, SL — superlattice, UD — undoped.

taking into account the finite depth of penetration of the electromagnetic field into the DBR, gives the value of the effective length of the cavity $\sim 2.4\,\mu$m. Detailed description of the heterostructure design and the VCSEL design is given in [6].

The current carrier injection efficiency η_{int} and the internal optical losses A_{int} can be found from the dependence of the external quantum efficiency of the laser η on the loss degree of radiation coupling A_m according to the expression $\eta = \eta_{int}/(1 + A_{int}/A_m)$. In this case, the total losses by the radiation coupling per one pass of a photon are given by the reflection coefficients of the totally reflecting mirror (R_B) and the output mirror (R_T) at the resonant wavelength of the microcavity as $A_m = -\ln\sqrt{R_T R_B}$. The A_m variation can be implemented both by changing the number of DBR [3,7] pairs and by changing the thickness of the near-surface layer of the output DBR [4,8]. However, in the first case, the number of possible variants is limited and requires either the preparing of several DBR wafers or precision etching of the given number of pairs of quarter-wave layers. The second approach requires the increased accuracy of etching of the near-surface GaAs layer, which, taking into account the strong dependence of the reflection coefficient on the layer thickness and the formation of natural oxide, increases the estimation error the A_m level. As alternative approach, one can consider the possibility of depositing on the surface of the output DBR the additional dielectric layer with lower refraction index. Figure 2 shows the results of calculating the reflection coefficient of the output GaAs/AlGaAs DBR with the variation in the thickness of the deposited Si_xN_y layer obtained in the framework of the transfer matrix method [2] with taking into account the dependence of the refraction indices on the wavelength [9]. For comparison, the same figure shows calculated values of the reflection coefficient for varying the number of pairs of GaAs/AlGaAs quarter-wave layers in the output DBR. It can be seen that the deposition of the dielectric layer on the surface of the extraction mirror makes it possible to effectively vary its reflectivity in a wide range and potentially provide more precise control of the loss level for the radiation coupling of VCSEL compared to varying the number of pairs of quarter-wave layers.

In wide-aperture lasers (in lasers with large TJ diameter), the main contribution to the level of internal optical losses is made by optical losses on free carriers and interband absorption [2]. However, in narrow-aperture lasers, along with the increase in losses depending on the light diffraction, the saturable absorber effect manifests itself, which was previously discovered in the WF-VCSEL in the spectral range $1.55\,\mu$m [10] and is due to a decrease in the transverse optical confinement for the fundamental fashion. The effect increases as the size of the BTJ mesa and/or the TJ etching depth decrease, and it also depends on the magnitude of the spectral detuning of the optical gain maximum and the resonant wavelength of the VCSEL. It should be noted that the TJ etching depth also affects the mode composition of the laser radiation: the greater the depth, the with smaller size of the BTJ mesa, the generation through the

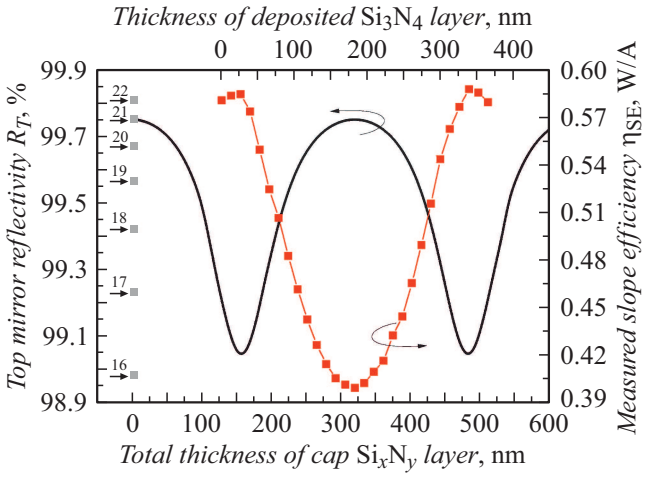

Figure 2. The calculated dependence of the reflection coefficient of the upper DBR based on 21 pairs of quarter-wave GaAs/AlGaAs layers on the thickness of the near-surface layer Si_xN_y and the experimental dependence of the differential efficiency η_{SE} at 20°C on the thickness of the deposited Si_xN_y layer. On the left, the symbols mark the calculated values of the reflection coefficient of the upper GaAs/AlGaAs DBR, achieved with different number of pairs.

fundamental mode (single-mode operation) is realized. For the WF-VCSEL under study in the spectral range 1.3 μm, the single-mode generation mode with the side-mode suppression factor > 40 dB over the entire range of operating currents is realized at the mesa size of the BTJ < 5 μm, while the effect of the saturable absorber, accompanied by jump-like increase in the output optical power with the pump current, is clearly manifested in lasers with the mesa size of the BTJ < 4 μm. At the same time, the analysis of the evolution of the ligth-current characteristics (LI-curves) of lasers with a change in temperature showed that the temperature stability of the characteristics of lasers with BTJ mesa size > 6 μm is mainly determined by the thermal ejection of carriers from the active region into the matrix and spectral detuning, whereas in lasers with BTJ mesa size < 5 μm, the additional mechanism is activated: the increase in the optical absorption of light at the resonant wavelength in the non-pumped parts of the active region and, as a consequence, the manifestation of the effect of the saturable absorber. In addition, in devices with a BTJ mesa size of > 7 μm, an increase in the differential efficiency with an increase in the pump current is observed in the initial section of the LI-curves, which, apparently due to the effect of the thermal lens, leading to the increase in the transverse optical confinement factor, and/or inhomogeneous pumping of the active region. For these reasons, in order to adequately estimate the level of internal optical losses caused by the design of the WF-VCSEL heterostructure, lasers with a BTJ mesa size in the range of 6−7 μm were chosen.

The external quantum efficiency η can be determined experimentally based on the LI-curves according to the expression $\eta = e\eta_{SE}/E_{ph}F_{out}$, where η_{SE} is differential efficiency, E_{ph} is energy of the emitted photon, e is electron charge, F_{out} is coefficient that takes into account the proportion of optical power output radiation through a particular mirror. The value estimation of the differential efficiency, which is defined as the rate of increase in the output optical power of a laser with a pump current in the lasing mode, was estimated in the linear region of the LI-curves near the lasing threshold, where thermal effects and gain nonlinearity at a high carrier density can be neglected. In order to minimize the fluctuations in instrumental characteristics depending on post-growth technology, instead of preparing series of VCSEL samples with different thicknesses of the dielectric layer, series of iterative measurements of the LI-curves was performed with step-by-step deposition of a dielectric layer of fixed thickness on the surface of the output DBR. For purposes of illustration of the effectiveness for this approach, Fig. 2 shows the dependence of the differential efficiency value at temperature of 20°C on the thickness of the deposited layer Si_xN_y for a WF-VCSEL with BTJ mesa size 6 μm.

Figure 3 shows the experimental dependences of the reciprocal external quantum efficiency on the reciprocal of the radiation output losses obtained at temperatures of 20 and 90°C. When calculating the η value, the losses of laser radiation part emerging through the substrate due to the finite value of the lower mirror reflectivity, were taken into account [2]. It should be noted that, by analogy with stripe-geometry lasers, when analyzing VCSELs, one often use the term of distributed losses α_{int} for outputting radiation, obtained by normalizing A_{int} to the effective length of the VCSEL microcavity L_{eff}. According to the linear approximation of the measured dependences with their subsequent extrapolation, the current injection efficiency at a temperature of 20°C reaches ∼ 76%, however, as the temperature increases to 90°C, η_{int} up to 64% In

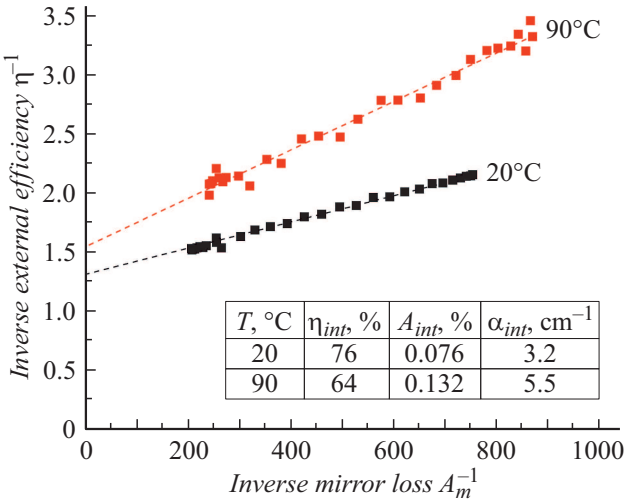

Figure 3. Experimental dependences of the reciprocal external quantum efficiency η^{-1} on the reciprocal of the output loss A_m^{-1} at temperatures of 20 and 90°C.

this case, for temperature of 20°C, the level of internal losses is $\sim 0.076\%$, which corresponds to distributed losses $\alpha_{int} \approx 3.2\,\mathrm{cm}^{-1}$. As the temperature increases to 90°C, A_{int} increases by more than 1.5 times up to $\sim 0.132\%$, which corresponds to $\alpha_{int} \approx 5.5\,\mathrm{cm}^{-1}$. The increase in internal optical losses with increasing temperature can be explained by an increase in absorption on free carriers and/or interband absorption, while the decrease in the efficiency of current injection, apparently is due to the thermal ejection of charge carriers from the active region and/or nonradiative recombination at the healed TJ heterointerface. More detailed analysis of the causes and mechanisms that determine the value and temperature behavior of the current carrier injection efficiency in a $1.3\,\mu$m WF-VCSEL with an active region based on an InGaAs/InGaAlAs superlattice requires further research. It should be noted that the presented level of internal optical losses is not only significantly lower than the published values for the WF-VCSEL in the spectral range $1.55\,\mu$m with n^+/p^+-InAlGaAs TJ and the active region based on thin InGaAs/InAlGaAs quantum wells (QWs) ($A_{int} \approx 0.214\%$ and $\alpha_{int} \approx 6.3\,\mathrm{cm}^{-1}$ at 20°C, $A_{int} \approx 0.309\%$ and $\alpha_{int} \approx 9.1\,\mathrm{cm}^{-1}$ at 85°C) [8] and for an WF-VCSEL in the spectral range $1.3\,\mu$m with n^+/p^+-InAlGaAs TJ and an active region based on thick InAlGaAs QWs ($A_{int} \approx 0.221\%$ and $\alpha_{int} \approx 9\,\mathrm{cm}^{-1}$ at 20°C, $A_{int} \approx 0.285\%$ and $\alpha_{int} \approx 11.6\,\mathrm{cm}^{-1}$ at 70°C) [4], but also comparable to the record low level of internal optical losses for hybrid VCSELs spectral range $1.55\,\mu$m with a short resonator, n^+-InGaAs/p^+-InAlGaAs TJ and an active region based on thick InAlGaAs QWs ($A_{int} \approx 0.13\%$ and $\alpha_{int} \approx 10\,\mathrm{cm}^{-1}$ at 35°C) [3]. Moreover, the obtained internal optical losses are comparable with the record low results for short-wavelength VCSELs both in geometry with carrier injection through doped mirrors ($A_{int} \approx 0.09\%$ and $\alpha_{int} \approx 6\,\mathrm{cm}^{-1}$ at 20°C) [11], and in geometry with carrier injection through intracavity contacts ($A_{int} \approx 0.072\%$ and $\alpha_{int} \approx 5\,\mathrm{cm}^{-1}$ at 20°C) [7].

In this way, the results of the analysis of efficiency for current injection and the level of internal optical losses of an WF-VCSEL in the spectral range $1.3\,\mu$m with the composite TJ n^+-InGaAs/p^+-InGaAs/p^+-InAlGaAs and the active region based on short-period InGaAs/InGaAlAs superlattice, are presented It is shown that the proposed VCSEL design provides the realizing low internal optical losses: A_{int} and α_{int}, respectively, less than 0.08% and $3.5\,\mathrm{cm}^{-1}$ at 20°C and less than 0.14% and $6.0\,\mathrm{cm}^{-1}$ at 90°C.

Conflict of interest

The authors declare that they have no conflict of interest.

References

[1] L.R. Chen, IEEE J. Light. Technol., **35** (4), 824 (2017). DOI:10.1109/JLT.2016.2613861

[2] *VCSELs: fundamentals, technology and applications of vertical-cavity surface emitting lasers*, ed. by R. Michalzik (Springer, Berlin, 2013). DOI: 10.1007/978-3-642-24986-0

[3] S. Spiga, W. Soenen, A. Andrejew, D.M. Schoke, X. Yin, J. Bauwelinck, G. Böhm, M.-C. Amann, J. Light. Technol., **35** (4), 727 (2017). DOI: 10.1109/JLT.2016.2597870

[4] D. Ellafi, V. Iakovlev, A. Sirbu, G. Suruceanu, Z. Mickovic, A. Caliman, A. Mereuta, E. Kapon, IEEE J. Sel. Top. Quant. Electron., **21** (6), 414 (2015). DOI: 10.1109/jstqe.2015.2412495

[5] S.A. Blokhin, M.A. Bobrov, N.A. Maleev, A.A. Blokhin, A.G. Kuz'menkov, A.P. Vasil'ev, S.S. Rochas, A.G. Gladyshev, A.V. Babichev, I.I. Novikov, L.Ya. Karachinsky, D.V. Denisov, K.O. Voropaev, A.S. Ionov, A.Yu. Egorov, V.M. Ustinov, Tech. Phys. Lett., **46** (9), 854 (2020). DOI: 10.1134/S1063785020090023

[6] S.A. Blokhin, A.V. Babichev, A.G. Gladyshev, L.Ya. Karachinsky, I.I. Novikov, A.A. Blokhin, S.S. Rochas, D.V. Denisov, K.O. Voropaev, A.S. Ionov, A.Yu. Egorov, Electron. Lett. (First published: 3 June 2021). DOI: 10.1049/ell2.12232

[7] G.M. Yang, M.H. MacDugal, V. Pudikov, P.D. Dapkus, IEEE Photon. Technol. Lett., **7** (11), 1228 (1995). DOI: 10.1109/68.473454

[8] S.A. Blokhin, M.A. Bobrov, A.A. Blokhin, A.G. Kuzmenkov, N.A. Maleev, V.M. Ustinov, E.S. Kolodeznyi, S.S. Rochas, A.V. Babichev, I.I. Novikov, A.G. Gladyshev, L.Ya. Karachinsky, D.V. Denisov, K.O. Voropaev, A.S. Ionov, A.Yu. Egorov, Opt. Spectrosc., **127** (1), 140 (2019). DOI: 10.1134/S0030400X1907004X.

[9] S. Adachi, J. Appl. Phys., **66** (12), 6030 (1989). DOI: 10.1063/1.343580

[10] S.A. Blokhin, M.A. Bobrov, A.A. Blokhin, A.P. Vasil'ev, A.G. Kuz'menkov, N.A. Maleev, S.S. Rochas, A.G. Gladyshev, A.V. Babichev, I.I. Novikov, L.Ya. Karachinsky, D.V. Denisov, K.O. Voropaev, A.S. Ionov, A.Yu. Egorov, V.M. Ustinov, Tech. Phys. Lett., **46** (12), 1257 (2020). DOI: 10.1134/S1063785020120172.

[11] S.A. Blokhin, N.A. Maleev, A.G. Kuzmenkov, A.V. Sakharov, M.M. Kulagina, Y.M. Shernyakov, I.I. Novikov, M.V. Maximov, V.M. Ustinov, A.R. Kovsh, S.S. Mikhrin, N.N. Ledentsov, G. Lin, J.Y. Chi, IEEE J. Quant. Electron., **42** (9), 851 (1989). DOI: 10.1109/JQE.2006.880125